symmetry

MDPI

Article

Design of a Hyperbolic Metamaterial as a Waveguide for Low-Loss Propagation of Plasmonic Wave

Ya-Chen Chang [1], Teh-Li Chan [2], Cheng-Chung Lee [1], Yi-Jun Jen [2,*] and Wei-Chieh Ma [2]

[1] Department of Optics and Photonics/Thin Film Technology Center, National Central University, 300, Chung Da Rd., Chung Li, Taoyuan 32001, Taiwan; 105286004@cc.ncu.edu.tw (Y.-C.C.); cclee@dop.ncu.edu.tw (C.-C.L.)

[2] Department of Electro-Optical Engineering, National Taipei University of Technology, Taipei 106, Taiwan; t104659002@ntut.edu.tw (T.-L.C.); t108658019@ntut.edu.tw (W.-C.M.)

* Correspondence: jyjun@ntut.edu.tw

Abstract: A stratiform hyperbolic metamaterial comprises multiple units of symmetrical metal-dielectric film, stacked to have a precisely equivalent refractive index, admittance, and iso-frequency curve. A metamaterial that is composed of stacks of symmetrical films as a waveguide to couple a diffracted wave into a horizontally propagating plasmonic wave is designed herein. By tuning the parameters of the constituent thin films within a hyperbolic metamaterial, both the loss of the plasmonic wave and admittance matching are minimized and optimized, respectively.

Keywords: hyperbolic; admittance; symmetrical film stack

check for updates

Citation: Chang, Y.-C.; Chan, T.-L.; Lee, C.-C.; Jen, Y.-J.; Ma, W.-C. Design of a Hyperbolic Metamaterial as a Waveguide for Low-Loss Propagation of Plasmonic Wave. *Symmetry* **2021**, *13*, 291. https://doi.org/10.3390/sym13020291

Academic Editor: Victor Borovkov
Received: 4 December 2020
Accepted: 6 February 2021
Published: 9 February 2021

Publisher's Note: MDPI stays neutral with regard to jurisdictional claims in published maps and institutional affiliations.

Copyright: © 2021 by the authors. Licensee MDPI, Basel, Switzerland. This article is an open access article distributed under the terms and conditions of the Creative Commons Attribution (CC BY) license (https://creativecommons.org/licenses/by/4.0/).

1. Introduction

Optical metamaterials are artificial subwavelength structures with extraordinary light–matter interaction properties that are not exhibited by natural materials [1]. Hyperbolic metamaterial (HMM) is an anisotropic material that has been widely studied owing to its unique hyperbolic dispersion [2]. The sign of the tangential permittivity opposes that of the vertical permittivity for transverse magnetic (TM) polarization mode. The iso-frequency curves (IFCs) of HMMs can be classified into two types by the signs of the tangential permittivity and the vertical permittivity. If the vertical permittivity is negative, then the medium is type-I, and if the tangential permittivity is negative, then the medium is type-II [3]. Type-I HMMs support the propagation of electromagnetic waves with both small and large wave vectors. Type-II HMMs support propagation only for electromagnetic waves with large wave vectors [4]. The unusual hyperbolic dispersion can be used in subwavelength diffraction-limited optical imaging [5–8], broadband optical absorption [9–11], high-resolution nanolithography [12–15], and spontaneous emission engineering [16].

Metamaterials with a near-zero effective permittivity, called epsilon-near-zero (ENZ) metamaterials, have attracted attention because of their many unusual phenomena, such as enhanced magnification and absorption [17], anti–Snell's law refraction [18], thermal emission control [19], a diffraction-free optical beam [20], biosensing [21], negative index [22], and subwavelength nanolithography [23]. The most common realization of effective hyperbolic dispersion and ENZ metamaterials is the metal-dielectric multilayered structure [24]. For a type-II HMM with its principal permittivity along the surface of approximately zero, the plasmonic wave would propagate horizontally. Placing such an HMM underneath a grating allows one high-ordered diffracted wave to be coupled into the HMM and to propagate with low loss [23]. The standing wave that is formed within the HMM then exhibits a subwavelength-scale periodic intensity variation, which is exploited in subwavelength lithography. To achieve hyperbolic dispersion, the components of the effective permittivity tensor must be negative in parallel or perpendicular to the anisotropic axis [25].

Generally, the electromagnetic properties of multilayer metamaterials can be simply and roughly described using the effective medium approximation (EMA) theory [26,27], which applies when the structures of the multilayer are much smaller than the wavelength. The EMA is an approximation method to have the principal permittivity for an anisotropic medium. The EMA assumes a permeability of unity. It can qualitatively describe the property of an HMM by neglecting the imaginary parts of principal permittivity values in the dispersion relation [25]. However, the equivalent permeability is not unity for most metal-dielectric composites because the localized surface plasmon resonance induces magnetic dipole moments between the densely packed metal clusters. Therefore, the optical properties of multilayer metamaterials cannot be completely predicted using the EMA, especially when the period or the thickness of the multilayer is subwavelength. In real application, we need a precise description for the equivalent refractive index and admittance that are varied with the direction of wave propagation. Relevant studies [28,29] have elucidated the performances and structures of HMMs, but their designs were not shown in detail. Furthermore, they have not considered loss due to admittance mismatching between the metamaterial structure and the incident medium.

For a layered metal-dielectric multilayer, a symmetrical film stack has an exact equivalent refractive index that is a function of the incident angle. Its equivalent admittance and refractive index may be independent of each other, so both the permittivity and the permeability of a typical metal-dielectric composite must be considered in determining its electromagnetic properties. The equivalent film stack is a model that is based on thin-film optics. In this work, a metal-dielectric multilayer that comprises multiple symmetrical film stacks is arranged as a hyperbolic metamaterial. The precise equivalent refractive index and admittance as functions of the angle of incidence are retrieved by calculating the characteristic matrixes of the constituent thin films. The equivalent refractive index is used to plot precise IFC of HMM. A method for designing a stratiform HMM that comprises symmetrical film stacks is then developed to enable an incident wave to be coupled into the HMM to propagate horizontally along the HMM waveguide. Both the equivalent refractive index and admittance are tailored to enable low-loss propagation and highly efficient light coupling. A previously presented example is considered herein with the purpose of improving loss with the proposed method.

2. Materials and Methods

For a metal-dielectric symmetrical film stack, the equivalent refractive index, equivalent intrinsic admittance, and refracted angle can be derived from the calculated characteristic film matrix and represented as $N_{eq}(\theta, \lambda, P_1, P_2 \ldots)$, $E_{eq}^{int}(\theta, \lambda, P_1, P_2 \ldots)$, and $\theta_{eq}(\theta, \lambda, P_1, P_2 \ldots)$, respectively, where θ is the angle of incidence, λ is wavelength of incident wave, and P_i are optical constants of each composite thin film including refractive index and thickness. To obtain N_{eq}, one of the multiple branches of the equivalent refractive index must be selected by imposing the requirement of continuity: the equivalent refractive index and the equivalent admittance of any film versus wavelength or thickness must be continuous [30]. According to the definition of the phasor of field $e^{\iota\omega t}$, the real part of the equivalent admittance has to be positive and the imaginary part of the equivalent refractive index must be negative [31,32]. The wave vector component k_z is given by

$$k_z = \frac{2\pi}{\lambda_0} N_{eq} \cos\theta_{eq}, \quad (1)$$

The component k_z as a function of θ can be represnted as the iso-frequency curves (IFCs) of a metamaterial, which plot the real part and imaginary part of k_z as functions of k_x. In plotting the IFCs, the values of k_x and k_z are normalized to $k_0 = 2\pi/\lambda$. The work of Xi Chen et al. is considered here, with IFC plotted using Equation (1). In their work [23], a type-II ENZ HMM made of seven layers of alternating 6 nm thick Al and 47 nm thick Al_2O_3 films was shown to have a near-zero principal permittivity in the direction parallel to the film surface. Therefore, the third-ordered diffracted wave from a grating

with $\lambda = 405$ nm and $k_x = 1.736k_0$ was coupled into a horizontally propagating wave in the HMM. The structure is a typical seven-layered metal (M)-dielectric (D) symmetrical film stack MDMDMDM. Figure 1 shows the equivalent model of the film stack. The refractive indices of Al and Al_2O_3 are 0.465–4.764i and 1.680, respectively, at a wavelength of 405 nm [23]. Figure 2 shows the IFCs of the proposed HMM, plotted using Equation (1). To obtain the IFCs over a wide range of k_x, the index of refraction of the cover medium is assumed to have a high value of ten. The refractive index of cover medium is set to be 10 in order to offer enough wave vector component k_x then the IFC can be plotted over a wide range of k_x. On the other hand, the index of cover medium should be large enough to cover several orders of diffracted waves as a grating. The precise IFC reveals the k_x that has minimum k_z for low-loss horizontally propagation of plasmonic wave. According to the k_x, the grating can be designed to offer a diffracted wave at a certain order that can propagate horizontally in the waveguide. In order to have the diffracted wave be coupled into the waveguide, the equivalent admittance including the substrate and the multilayered waveguide is considered to have highly efficient light coupling and propagation.

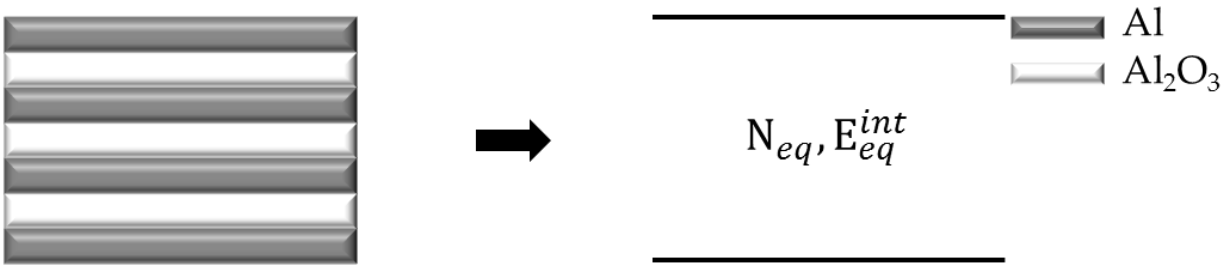


Figure 1. The equivalent model of the film stack MDMDMDM. M, metal; D, dielectric.

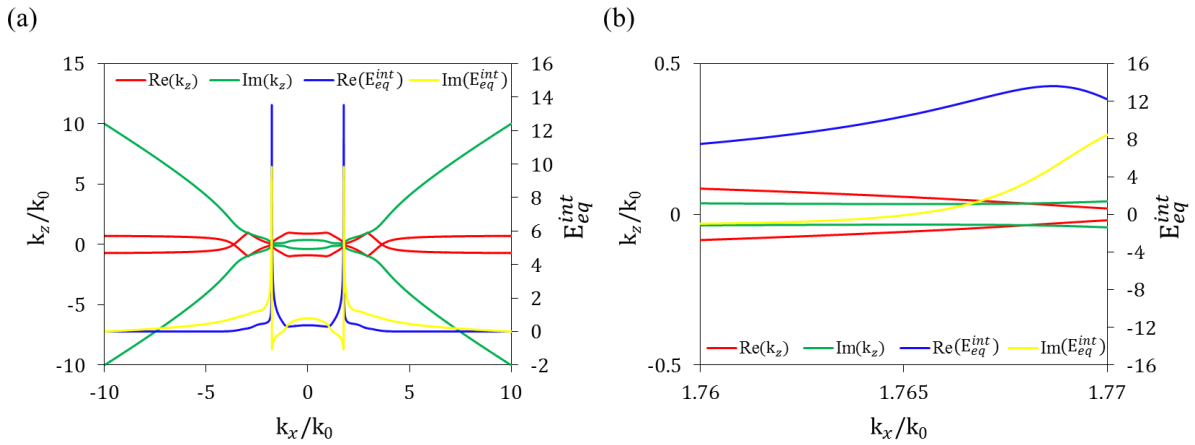


Figure 2. (**a**) Iso-frequency curves and admittance of seven-layered structure composed of 6 nm thick Al and 47 nm thick Al_2O_3 films. (**b**) Iso-frequency curves and admittance around $k_z = 0$.

Figure 2 presents real and imaginary parts of k_z/k_0 represented as $Re(k_z/k_0)$ and $Im(k_z/k_0)$ versus k_x/k_0, respectively. The equivalent admittance E_{eq}^{int} versus k_x/k_0 is also shown in Figure 2. The IFC of the real part of k_z is not as hyperbolic as in the work of Xi Chen et al. [23]. For the equivalent admittance E_{eq}^{int} versus k_x/k_0, the two minima points of $Re(k_z/k_0)$ are at $k_x = 1.774k_0$ and $k_x = 3.646k_0$. The small real part of k_z accompanies large variation of admittance. The sharp peaks of the real and imaginary parts of admittance are at $k_x = 1.769k_0$ and $k_x = 1.772k_0$, respectively. Coupling light into the HMM layer with a large imaginary part of admittance by arranging admittance matching layers adjacent to the HMM is difficult. In the work of Xi Chen et al. [23], the grating is designed to support light coupling at $k_x = 1.736k_0$ where, according to our calculation, the wave vector $k_z = (0.164 - 0.051i)k_0$ and the admittance $E_{eq}^{int} = 3.922 - 0.878i$. However,

k_x is better for light coupling and propagation within the range of k_x/k_0 from 1.762 to 1.765, where the wave vector k_z varies from $(0.077 - 0.035i)k_0$ to $(0.056 - 0.034i)k_0$ and the admittance varies from 8.240–0.869i to 10.677 + 0.064i. The loss within the HMM herein is lower than obtained previously [23] because the imaginary part of k_z and the imaginary part of the admittance are smaller.

Analysis reveals that an HMM that is composed of alternating metal (denoted as M) and dielectric (denoted as D) films should have the symmetrical form MDMMD . . . MMDM = $(MDM)^m$, where m is the number of symmetrical stacks, or DMDDM . . . DDMD = $(DMD)^m$. In both cases, (MDM) or (DMD) is the unit cell in the HMM. Therefore, a basic design for HMM involves the stacking of several cells. The E_{eq}^{int} and the k_z versus k_x of a multiple cell structure are determined by the unit cell and do not vary with the number of cells. However, in practical applications, whether the system can couple more light into the HMM depends on the layers and medium adjacent to it. Therefore, admittance-matching for the system depends on the number of cells within the HMM. Tuning the cell number is similar to tuning the thickness of an optical coating for antireflection.

Herein, a procedure for designing a multiple DMD film stack for a horizontal propagating waveguide with low loss is proposed, as shown in Figure 3. The thicknesses of the dielectric film and metal film are denoted as d_D and d_M, respectively. First, the materials of the dielectric layer and the metal layer are selected for a reference wavelength. In order to compare our method with the previous work, the thickness of the metal film in our example is the same as the case in the literature [23].

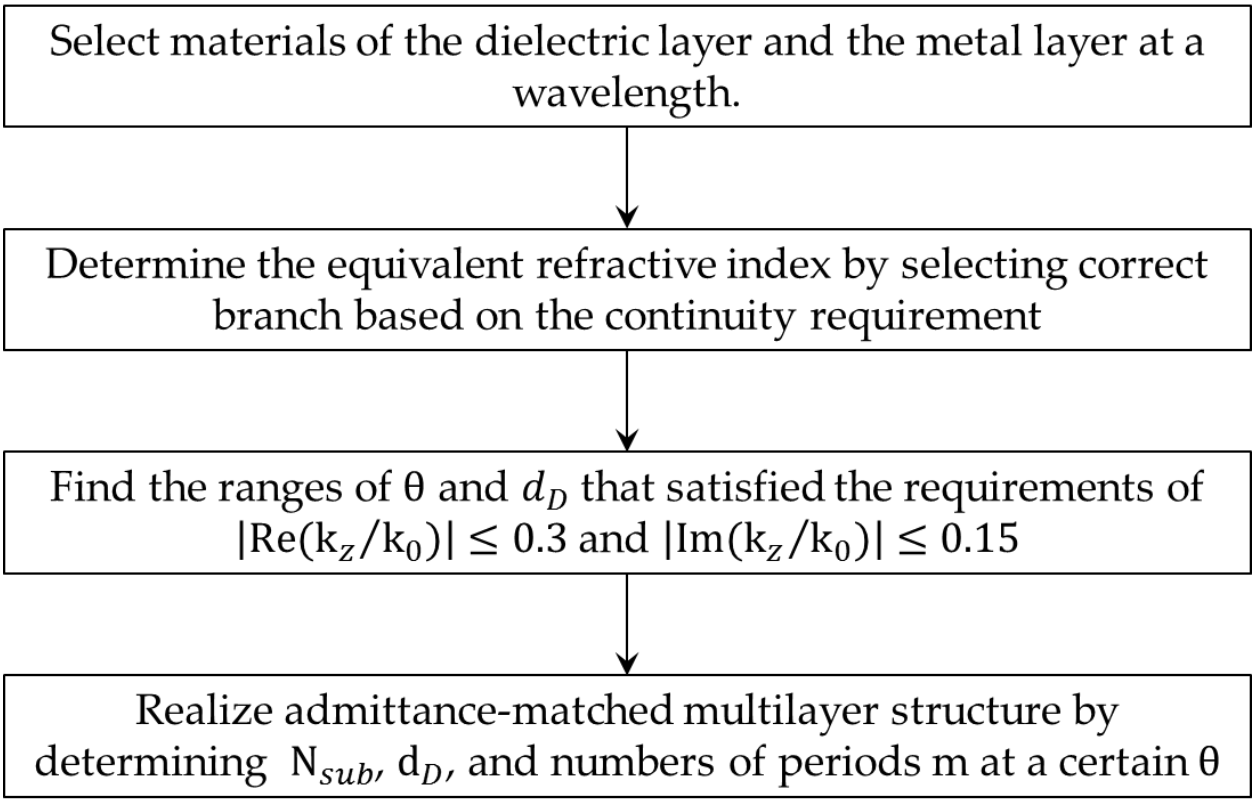


Figure 3. Flow chart of design method for hyperbolic metamaterial (HMM) plasmonic waveguide.

3. Results

With the equivalent refractive index, both the real part and the imaginary part of k_z/k_0 versus θ and d_D are plotted to identify the region that corresponds to small magnitudes of $Re(k_z/k_0)$ and $Im(k_z/k_0)$. The ranges of θ and d_D that satisfy the requirements that both $|Re(k_z/k_0)|$ and $|Im(k_z/k_0)|$ are close to zero are then calculated. For a horizontally

propagating wave, the angle of incidence θ is fixed and d_D is varied to achieve admittance matching. Whether the unit cells can be stacked for admittance matching depends on the equivalent refractive index, admittance, and refractive index of the substrate. In thin-film optics [33], the equivalent admittance Y_{eq} under the top surface of a multilayer on a substrate can be obtained from the product of all characteristic film matrixes; the E_{eq}^{int} and Y_{eq} are different. Figure 4 shows the system for design. The $E_{eq}^{int}(\theta, \lambda, P_1, P_2 \ldots)$ represents the equivalent intrinsic admittance of a symmetrical film stack. It means that the symmetrical film stack can be equivalent to a layer with admittance $E_{eq}^{int}(\theta, \lambda, P_1, P_2 \ldots)$. For a multilayered system, thin films and substrate under the top surface can be equivalent to a medium with admittance of Y_{eq}. When Y_{eq} equals the refractive index of the cover medium N_{inc}, admittance matching is realized and reflection is eliminated. Therefore, the period of the unit cell is increased, varying the equivalent admittance Y_{eq} of the whole structure under the top surface including the substrate with refractive index of N_{sub} under the multilayer. The optimal thickness, d_D, and number of periods, m, for which Y_{eq} is the closest to N_{inc} are most often chosen. The different equivalent refractive index N_{eq} and admittance E_{eq} indicate that the equivalent permeability departs from unity because the equivalent permittivity ε_{eq} and permeability μ_{eq} can be derived from the relationships: $\varepsilon_{eq} = E_{eq}N_{eq}$, $\mu_{eq} = N_{eq}/E_{eq}$.

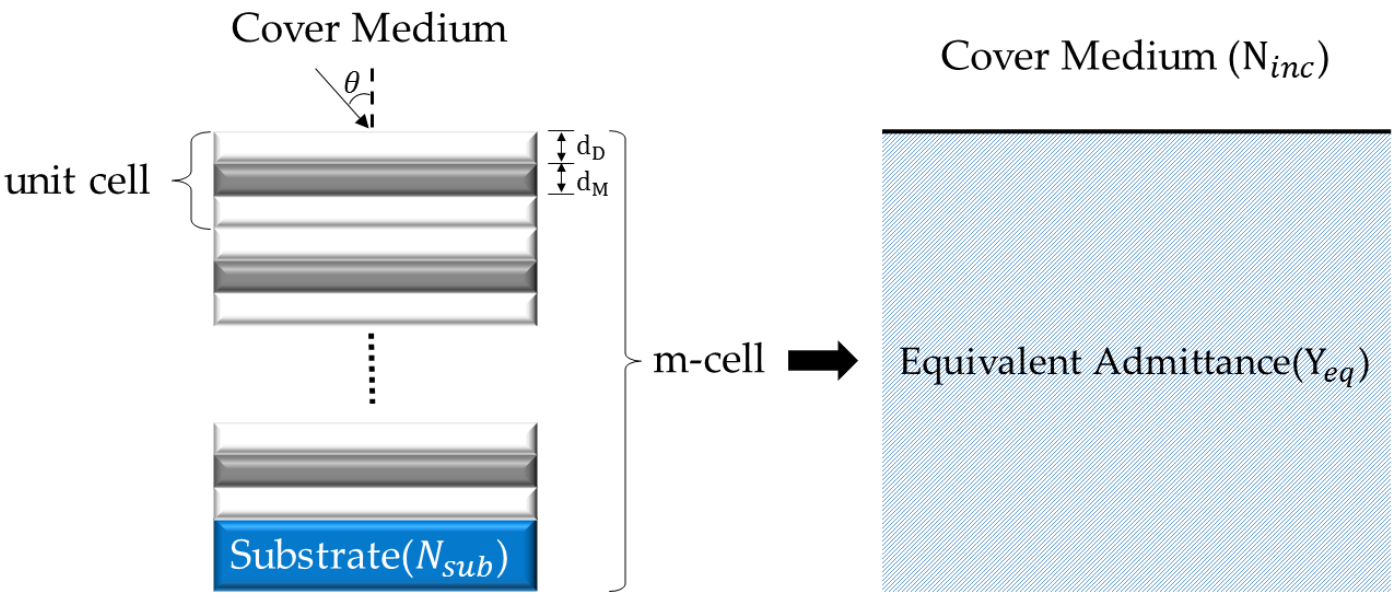


Figure 4. The system of m cells of DMD for design.

An aforementioned case of alternating Al and Al_2O_3 films was modified to provide an example of a multiple DMD design, such that the thickness of the Al layer was 6 nm. The complex value of k_z/k_0 was then calculated with the thickness of the Al_2O_3 layer from 0 to 90 nm and the incident angle from 0° to 90° using the equivalent refractive index of the correct branch. The black color in Figure 5 indicates the ranges of θ and d_D that satisfy the conditions of $|\mathrm{Re}(k_z/k_0)| \leq 0.3$ and $|\mathrm{Im}(k_z/k_0)| \leq 0.15$. The criteria used for this figure are the upper limits for both the real part and the imaginary part of k_z. Our purpose is to fine the minimum magnitude of k_z to ensure the horizontal propagation and low loss. A wide range of thicknesses of the Al_2O_3 layer from 22.9 to 63.4 nm satisfies these conditions at $\theta = 10$. An incident wave at $\theta = 10$ in a cover medium with $N_{inc} = 10$ is considered to offer a wave vector component of $k_x = 1.736k_0$, so the incident light wave is coupled into a horizontally propagating wave. Next, the variations of admittance Y_{eq} with N_{sub} and d_D were calculated for different numbers of periods m. N_{sub} was varied in the range of 1.4–1.73 that can be easily achieved by arranging dielectric films on a transparent substrate. Figure 6 shows the absolute difference between the equivalent admittance Y_{eq} and the refractive

index of the cover medium N_{inc} for possible N_{sub}, d_D, and numbers of periods, m. The dark blue areas in Figure 6 represent a difference $|Y_{eq} - N_{inc}|$ of less than 0.5: $|Y_{eq} - N_{inc}|$ is less than 0.5 only at m = 6. The optimal structure is obtained with $N_{inc}/(DMD)^6/N_{sub}$ with 6 nm thick Al (M), 25.6 nm thick Al_2O_3 (D), and N_{sub} of 1.474. Figure 7 plots the IFCs. The k_z/k_0 at $k_x = 1.736k_0$ is 0.140–0.100i, of which the imaginary part is less than that of the previously presented seven-layered structure. The Y_{eq} is 10.077–0.100i, indicating good admittance matching to $N_{inc} = 10$. The wave vector component $k_x = 1.736k_0$ in Figure 7 is near the wave vector of surface plasmon wave excited at the interface between Al and Al_2O_3 that is presented as $k_{sp} = \sqrt{(\varepsilon_D)(\varepsilon_M)/(\varepsilon_D + \varepsilon_M)} = 1.789 + 0.024i$, where ε_M and ε_D are $-22.476 + 4.429i$ and 2.822 at 405 nm, respectively. Since the metal film is pretty thin, the loss within the metal is small. It is a collective response of all surface plasmon polaritons on each of the interfaces.

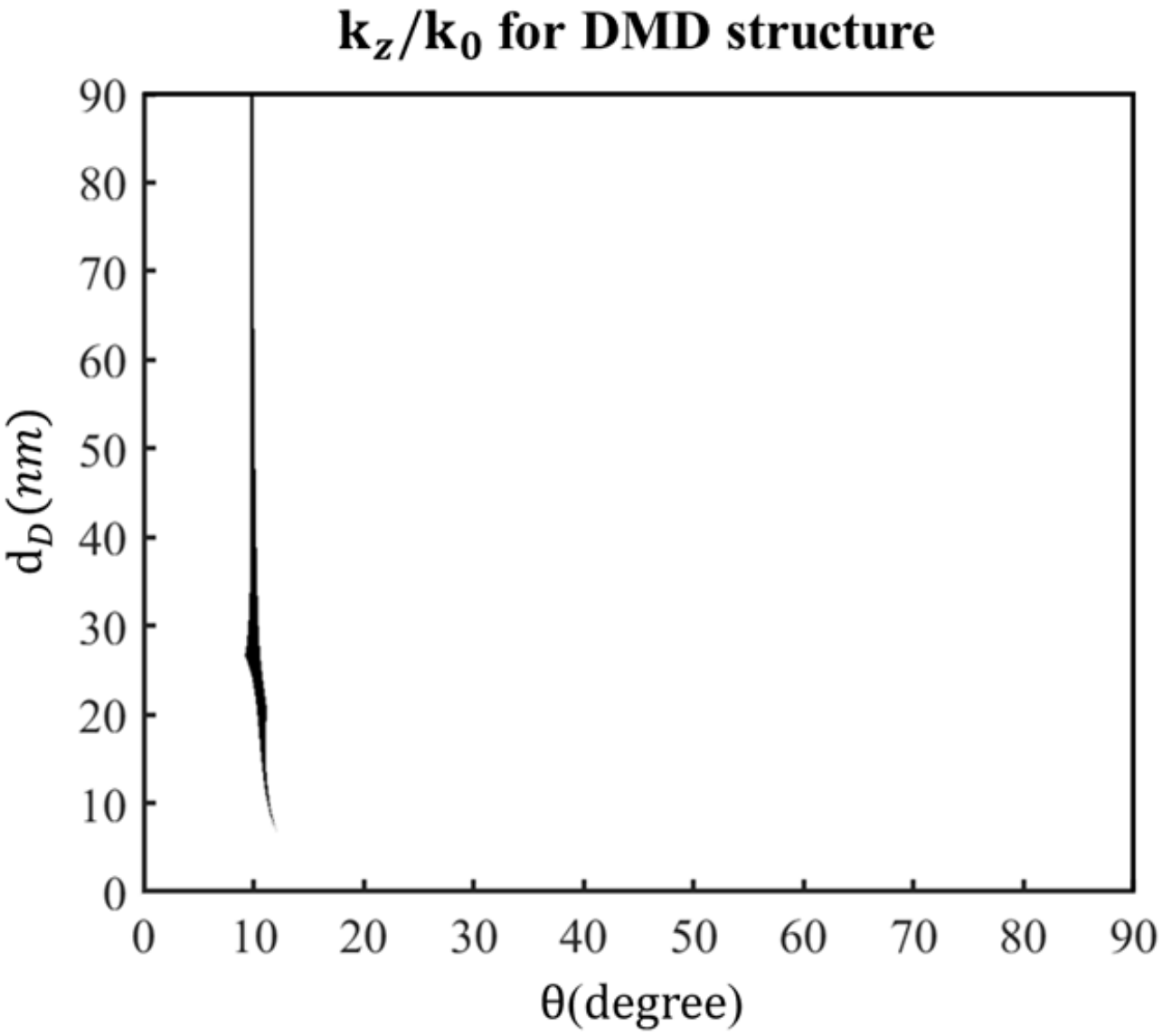


Figure 5. Ranges of θ and d_D for near-zero k_z .

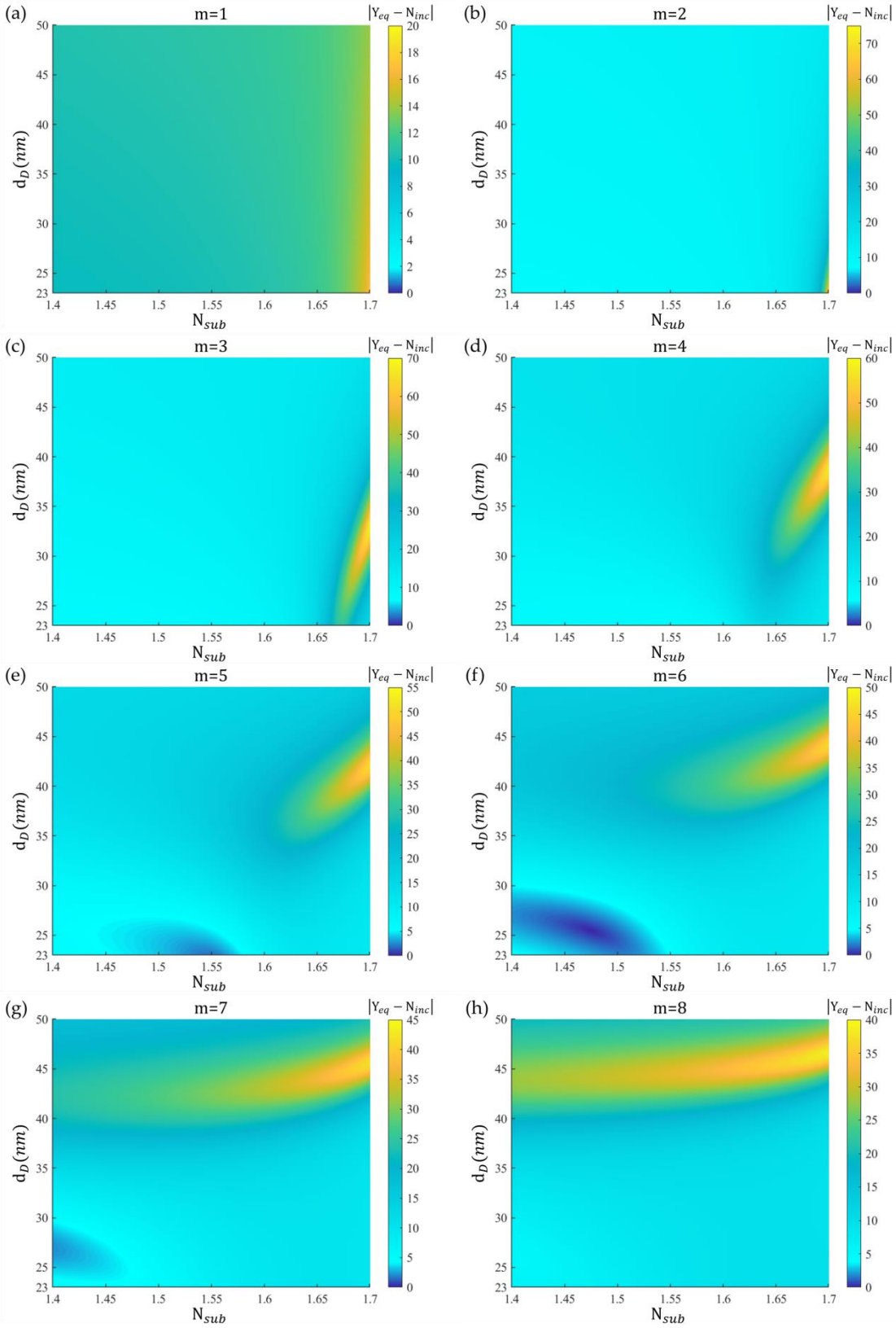


Figure 6. Admittance difference $\left|Y_{eq} - N_{inc}\right|$ for possible N_{sub}, d_D, and numbers of periods m from (**a**) m = 1 to (**h**) m = 8.

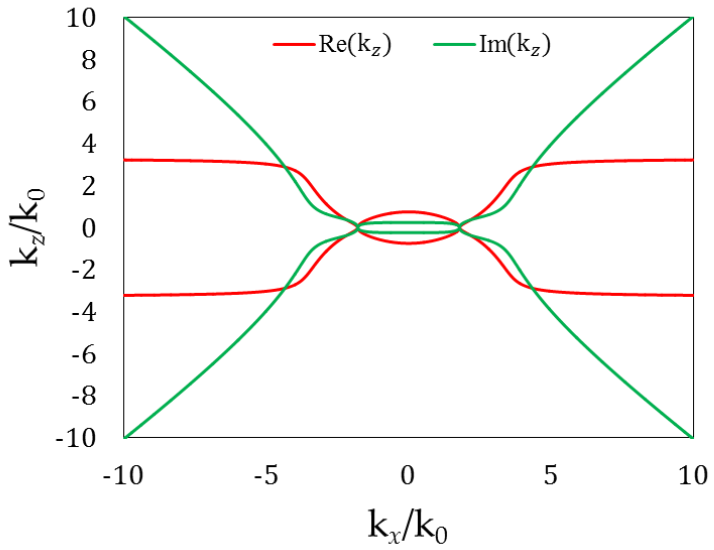


Figure 7. Iso-frequency curves (IFCs) of DMD unit cell.

4. Discussion

In this work, the optical property of an HMM is precisely controlled by arranging the HMM as a multiple symmetrical film stack. From the equivalent refractive index and admittance, the precise IFC can be plotted and an HMM that can efficiently couple diffracted light from gratings to horizontally propagating waves is thus developed. The proposed design method involves a layered configuration that can provide highly efficient light coupling and the low-loss propagation of a coupled wave. The proposed method can be extended to any metal and dielectric materials that are used to form an HMM to guide a plasmonic wave. The three-layered structure can be extended to a five- or seven-layered symmetrical film stack to offer more flexibility in design by tuning more parameters of the constituent thin films.

Author Contributions: Y.-J.J. conceived the initial idea of the design method. Y.-J.J. supervised the whole work with C.-C.L., Y.-C.C., T.-L.C. and W.-C.M. wrote the program and performed calculation. Y.-C.C., T.-L.C., C.-C.L. and Y.-J.J. analyzed and optimized the result. Y.-J.J. and Y.-C.C. wrote the article. All authors have read and agreed to the published version of the manuscript.

Funding: This research was funded by the Ministry of Science and Technology of the China, Taiwan, for financially supporting this research under contract MOST108-2221-E-027-100-MY3.

Institutional Review Board Statement: Not applicable.

Informed Consent Statement: Not applicable.

Data Availability Statement: The data presented in this study are available on request from the corresponding author.

Conflicts of Interest: The authors declare no conflict of interest.

References

1. Cai, W.; Shalaev, V.M. *Optical Metamaterials*; Springer: Berlin, Germany, 2010; Volume 10.
2. Poddubny, A.; Iorsh, I.; Belov, P.; Kivshar, Y. Hyperbolic metamaterials. *Nat. Photonics* **2013**, *7*, 948–957. [CrossRef]
3. Peragut, F.; Cerutti, L.; Baranov, A.; Hugonin, J.; Taliercio, T.; Wilde, Y.D.; Greffet, J. Hyperbolic metamaterials and surface plasmon polaritons. *Optica* **2017**, *4*, 1409–1415. [CrossRef]
4. Huo, P.; Zhang, S.; Liang, Y.; Lu, Y.; Xu, T. Hyperbolic Metamaterials and Metasurfaces: Fundamentals and Applications. *Adv. Opt. Mater.* **2019**, *7*, 1801616. [CrossRef]
5. Lee, H.; Liu, Z.; Xiong, Y.; Sun, C.; Zhang, X. Development of optical hyperlens for imaging below the diffraction limit. *Opt. Express* **2007**, *15*, 15886–15891. [CrossRef]
6. Liu, Z.; Lee, H.; Xiong, Y.; Sun, C.; Zhang, X. Far-field optical hyperlens magnifying sub-diffraction-limited objects. *Science* **2007**, *315*, 1686. [CrossRef]

7. Rho, J.; Ye, Z.; Xiong, Y.; Yin, X.; Liu, Z.; Choi, H.; Bartal, G.; Zhang, X. Spherical hyperlens for two-dimensional sub-diffraction imaging at visible frequencies. *Nat. Commun.* **2010**, *1*, 1–5. [CrossRef]
8. Lu, D.; Liu, Z. Hyperlenses and metalenses for far-field super-resolution imaging. *Nat. Commun.* **2012**, *3*, 1–9. [CrossRef] [PubMed]
9. Cui, Y.; Fung, K.H.; Xu, J.; Ma, H.; Jin, Y.; He, S.; Fang, N.X. Ultrabroadband light absorption by a sawtooth anisotropic metamaterial slab. *Nano Lett.* **2012**, *12*, 1443–1447. [CrossRef]
10. Riley, C.T.; Smalley, J.S.; Brodie, J.R.; Fainman, Y.; Sirbuly, D.J.; Liu, Z. Near-perfect broadband absorption from hyperbolic metamaterial nanoparticles. *Proc. Natl. Acad. Sci. USA* **2017**, *114*, 1264–1268. [CrossRef] [PubMed]
11. Landy, N.I.; Sajuyigbe, S.; Mock, J.J.; Smith, D.R.; Padilla, W.J. Perfect metamaterial absorber. *Phys. Rev. Lett.* **2008**, *100*, 207402. [CrossRef] [PubMed]
12. Xu, T.; Zhao, Y.; Ma, J.; Wang, C.; Cui, J.; Du, C.; Luo, X. Sub-diffraction-limited interference photolithography with metamaterials. *Opt. Express* **2008**, *16*, 13579–13584. [CrossRef] [PubMed]
13. Yang, X.; Zeng, B.; Wang, C.; Luo, X. Breaking the feature sizes down to sub-22 nm by plasmonic interference lithography using dielectric-metal multilayer. *Opt. Express* **2009**, *17*, 21560–21565. [CrossRef] [PubMed]
14. Zhu, P.; Shi, H.; Guo, L.J. SPPs coupling induced interference in metal/dielectric multilayer waveguides and its application for plasmonic lithography. *Opt. Express* **2012**, *20*, 12521–12529. [CrossRef] [PubMed]
15. Liang, G.; Chen, X.; Zhao, Q.; Guo, L.J. Achieving pattern uniformity in plasmonic lithography by spatial frequency selection. *Nanophotonics* **2018**, *7*, 277–286. [CrossRef]
16. Poddubny, A.N.; Belov, P.A.; Kivshar, Y.S. Spontaneous radiation of a finite-size dipole emitter in hyperbolic media. *Phys. Rev. A* **2011**, *84*, 023807. [CrossRef]
17. Jin, Y.; Xiao, S.; Mortensen, N.A.; He, S. Arbitrarily thin metamaterial structure for perfect absorption and giant magnification. *Opt. Express* **2011**, *19*, 11114–11119. [CrossRef]
18. Feng, S. Loss-induced omnidirectional bending to the normal in ϵ-near-zero metamaterials. *Phys. Rev. Lett.* **2012**, *108*, 193904. [CrossRef]
19. Dyachenko, P.N.; Molesky, S.; Petrov, A.Y.; Störmer, M.; Krekeler, T.; Lang, S.; Ritter, M.; Jacob, Z.; Eich, M. Controlling thermal emission with refractory epsilon-near-zero metamaterials via topological transitions. *Nat. Commun.* **2016**, *7*, 1–8. [CrossRef]
20. Sun, L.; Yang, X.; Wang, W.; Gao, J. Diffraction-free optical beam propagation with near-zero phase variation in extremely anisotropic metamaterials. *J. Opt.* **2015**, *17*, 035101. [CrossRef]
21. Yoo, D.; Nguyen, N.-C.; Martín Moreno, L.; Mohr, D.A.; Carretero-Palacios, S.; Shaver, J.; Peraire, J.; Ebbesen, T.W.; Oh, S.-H. High-Throughput Fabrication of Resonant Metamaterials with Ultrasmall Coaxial Apertures via Atomic Layer Lithography. *Nano Lett.* **2016**, *16*, 2040–2046. [CrossRef]
22. Gómez-Castaño, M.; Zheng, H.; García-Pomar, J.L.; Vallée, R.; Mihi, A.; Ravaine, S. Tunable index metamaterials made by bottom-up approaches. *Nanoscale Adv.* **2019**, *1*, 1070–1076. [CrossRef]
23. Chen, X.; Zhang, C.; Yang, F.; Liang, G.; Li, Q.; Guo, L.J. Plasmonic lithography utilizing epsilon near zero hyperbolic metamaterial. *ACS Nano* **2017**, *11*, 9863–9868. [CrossRef] [PubMed]
24. Wood, B.; Pendry, J.; Tsai, D. Directed subwavelength imaging using a layered metal-dielectric system. *Phys. Rev. B* **2006**, *74*, 115116. [CrossRef]
25. Ferrari, L.; Wu, C.; Lepage, D.; Zhang, X.; Liu, Z. Hyperbolic metamaterials and their applications. *Prog. Quantum Electron.* **2015**, *40*, 1–40. [CrossRef]
26. Bergman, D.J. The dielectric constant of a composite material—A problem in classical physics. *Phys. Rep.* **1978**, *43*, 377–407. [CrossRef]
27. Popov, V.; Lavrinenko, A.V.; Novitsky, A. Surface waves on multilayer hyperbolic metamaterials: Operator approach to effective medium approximation. *Phys. Rev. B* **2018**, *97*, 125428. [CrossRef]
28. Sukham, J.; Takayama, O.; Mahmoodi, M.; Sychev, S.; Bogdanov, A.; Tavassoli, S.H.; Lavrinenko, A.V.; Malureanu, R. Investigation of effective media applicability for ultrathin multilayer structures. *Nanoscale* **2019**, *11*, 12582–12588. [CrossRef] [PubMed]
29. Mahmoodi, M.; Tavassoli, S.H.; Takayama, O.; Sukham, J.; Malureanu, R.; Lavrinenko, A.V. Existence Conditions of High-k Modes in Finite Hyperbolic Metamaterials. *Laser Photon. Rev.* **2019**, *13*, 1800253. [CrossRef]
30. Jen, Y.J.; Liu, W.C. Design a Stratiform Metamaterial with Precise Optical Property. *Symmetry* **2019**, *11*, 1464. [CrossRef]
31. Kildishev, A.V.; Cai, W.; Chettiar, U.K.; Yuan, H.K.; Sarychev, A.K.; Drachev, V.P.; Shalaev, V.M. Negative refractive index in optics of metal–dielectric composites. *J. Opt. Soc. Am. B* **2006**, *23*, 423–433. [CrossRef]
32. Jen, Y.J.; Lakhtakia, A. Response to "Comment on 'Silver/silicon dioxide/silver sandwich films in the blue-to-red spectral regime with negative-real refractive index" Appl. *Phys. Lett.* **2012**, *101*, 156101.
33. Macleod, H.A. *Thin-Film Optical Filters*, 3rd ed.; Institute of Physics Publishing: Bristol, UK, 1986.